(4)

MEASUREMENTS OF THE WIGGLER'S MAGNETIC FIELD AND PARAMETERS FIXING FOR THE EL-OP SIMULATIONS.

15-June-1997

by

A. Gover, ,Y. Pinhasi, A. Arensburg

In this report we present the results of measurements of the magnetic field along the axis of the wiggler and a procedure to determine the saturation fields for the El-Op simulation.

Measurements of wiggler length:

The wiggler is composed of two entrance magnet pairs, 26 periods of 4 magnet pairs arranged in a Halbach configuration and 3 exit magnet pairs as shown in Fig. 1. The wiggler period is 44.44 mm. The total calculated length of the wiggler is

17.17 1155.44 2 8.27

Entrance 11.11 Periods Exit 11.11 Total

$(5.555+0.5-\cancel{5.555}) + 26x4x11.11 + (11.11 + \cancel{5.555}+0.5+5.555) = 1200.88mm$

Recent measurements of the wiggler dimensions with a caliper (M. Kanter, May 1997) confirm these results, except that an unintended space of *0.5mm* (more accurately *0.4mm* on the *+y* side and *0.6mm* on the *-y* side) was detected between the period magnets and the detachable exit magnet assembly. Consequently, the total wiggler length that was measured end-to- end, *1201.5mm* is consistent with the calculated length to a *0.12 mm* accuracy (see Fig. 2).

Measurements:

The measurement of the magnetic field of the wiggler's components was designed by M. Kanter and carried out with a high precision Hall probe model 9900 with two axis probe type A99-1808, borrowed from Soreq NRC. We made 4 measurements of the vertical (*y*) component of the magnetic field along the axis of the following magnet systems:

1. The entire wiggler as it was removed from the Tandem after the last opening.
2. The entrance magnets assembly alone
3. The exit magnets assembly alone
4. A pair of longitudinal magnets (gradient measurement)

The distances of the centers of the entrance and exit magnets from the axis, for the 3 first cases above, are shown in table 1.
When we made the measurement of the entire wiggler (case 1), the distances were according to the listing in column 1.

When we made the measurement of the separate entrance and exit magnets (cases 2 and 3), the distances were re-adjusted according to the listing of column 2 and 3 that were considered to be optimal after analyzing case 1 (Note: these distances are not final

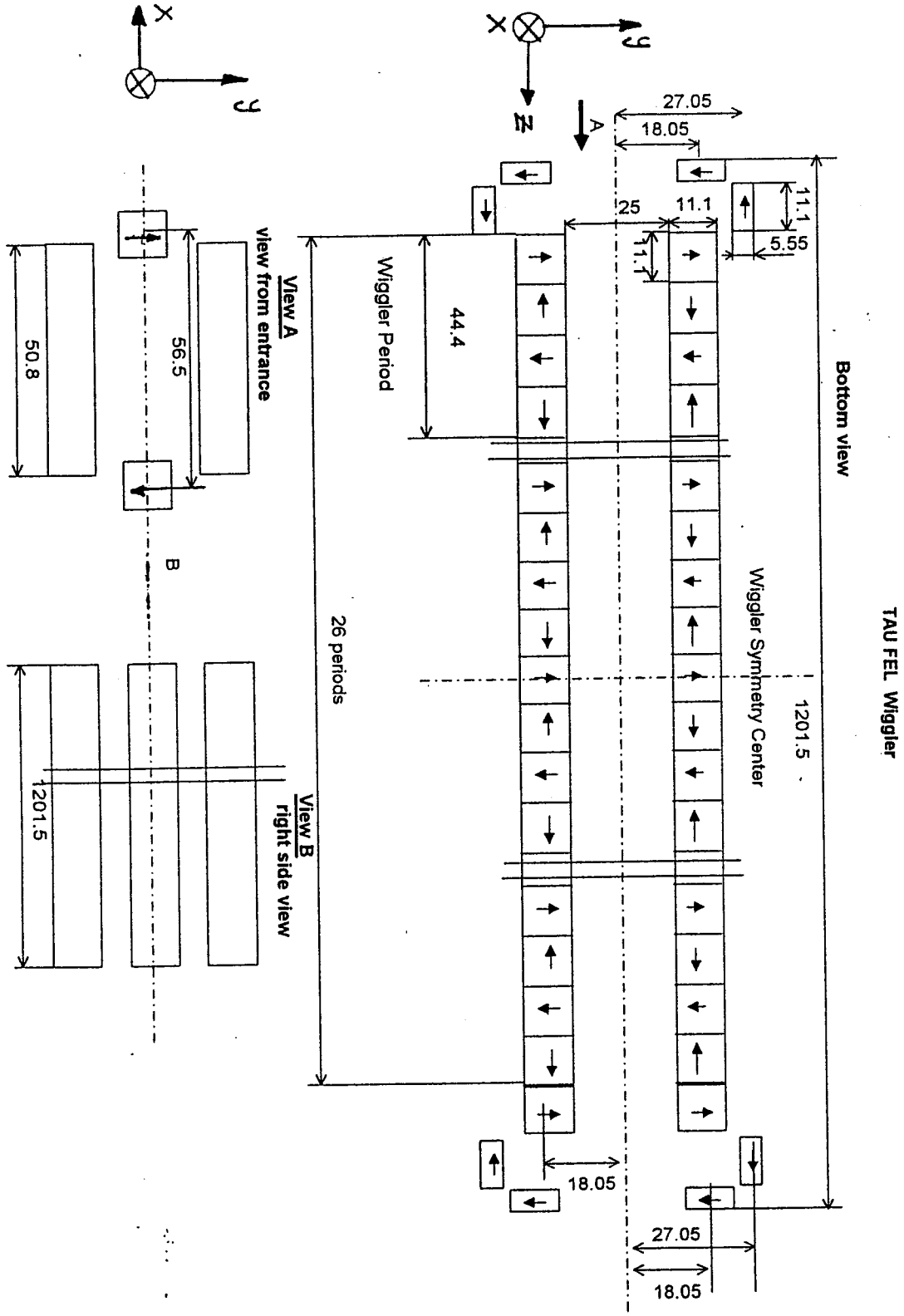

Figure 1: Schematic view of the Tandem FEL planar wiggler. The location of the entrance and exit magnets correspond to an old optimization of El-Op.

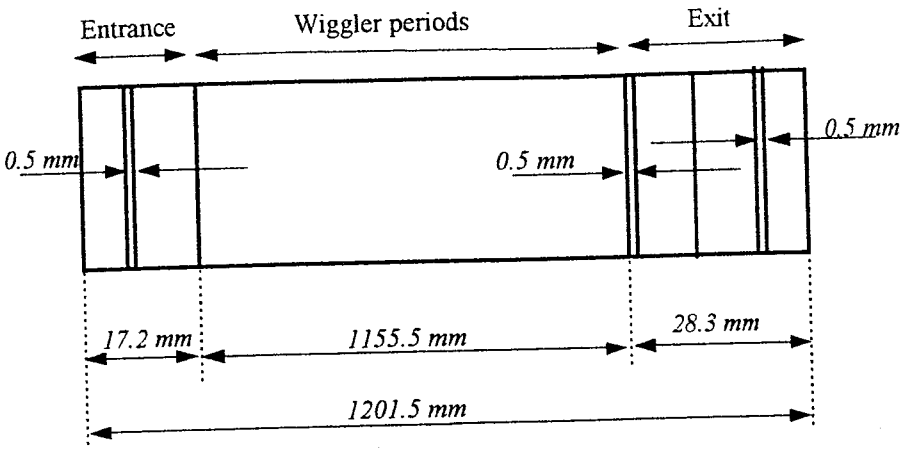

Figure 2: Wiggler dimensions

Table 1

	meas. 1 (on the wiggler)*	meas. 2 (entrance alone)**	meas. 3 (exit alone)**
Entrance			
d1.	18.05 mm	14.35 mm	
d2.	27.05 mm	31.05 mm	
Exit			
d1.	18.05 mm		18.05 mm
d2.	27.05 mm		31.05 mm
d3.	18.05 mm		14.35 mm

* from Ilya'r report from 3/3/97.
** recently updated results.

The results of the measurements are shown graphically in Fig's. 3,4 and 5 below. The Hall probe we used has a measurement tiphead with 0.5 mm length and a measurement accuracy of *1mG* in the lower range. Fields of the order of *1kG* were measured with a *0.1G* accuracy. The coincidence of the motion of the Hall probe with the wiggler's symmetry axis during the measurements is of the submillimeter order of magnitude. Therefore we assume that the measurements are accurate enough so that it is reasonable to adjust the simulation parameters by trying to fit the curve of the calculated magnetic field along the axis to the measured curves of Fig's 3,4 and 5.

For this purpose it was necessary to write a computer code that transforms one set of results so that the points at which the field is given in this set are equated to those of the second set, and so they can be compared. In our case the entire wiggler was measured at *1mm* intervals and we could produce a simulation with the same spatial resolution. However, in the case of the entrance and exit magnets, the measurements were not taken with equal spacing along the *z* axis, therefore the code is necessary. The function was written by A. Abramovich in the Matlab Language and is called "***matchaxi.m***". The parameters (saturation fields) adjustment procedure is done as follows:

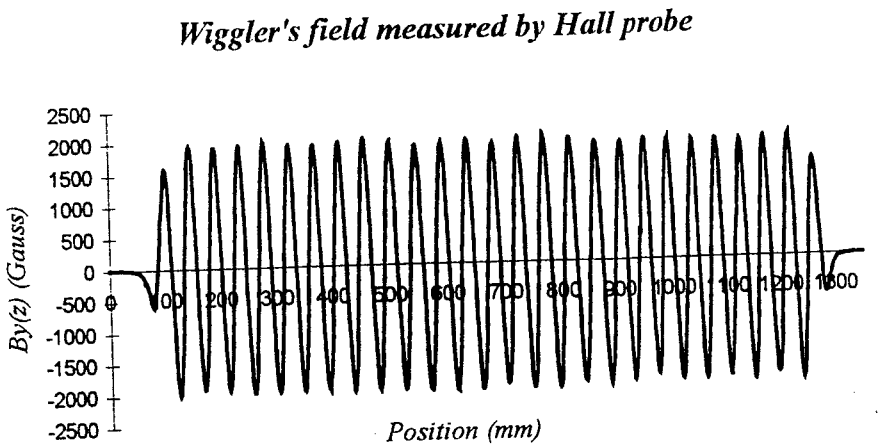

Figure 3: configuration 1, entire wiggler.

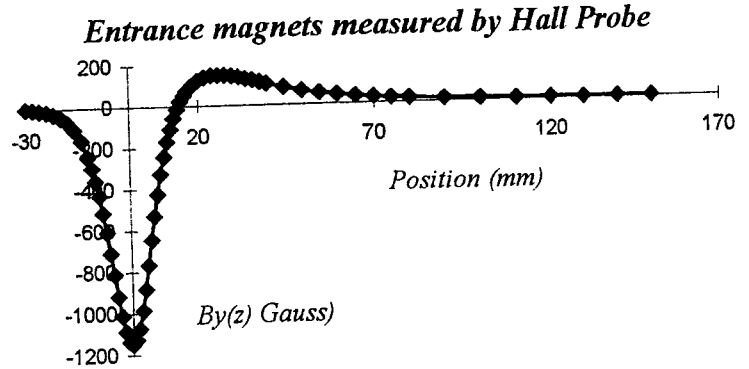

Figure 4: configuration 2, entrance magnets.

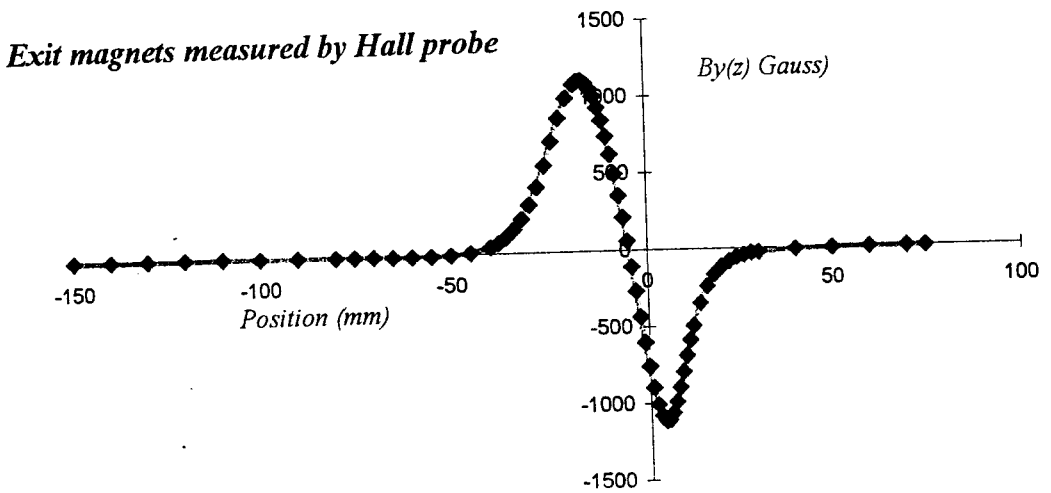

Figure 5: configuration 3, exit magnets.

Determination of the saturating fields for entrance and exit magnets

1. The magnetic measurements are done on some chosen geometry (position of the magnets relative to the axis). The dimensions are given in table 1 cols. 2 and 3. The measurements are done along the z axis with $x=y=0$.
2. A simulation is done with the magnets arranged with the same geometry as in the measurement. We produce n points.
3. The ***matchaxi*** function is applied to the two sets of results so that the z axis of the measurement set is matched to that of the simulation. We obtain the measured field $B_m(z_i)$ and the calculated field $B_c(z_i)$ at the points z_i with $i=1...n$. Note that in the simulation $B_c(z_i)$ is a linear function of the saturating field B_s.
4. For a certain choice of saturation fields, we determine the similarity between the shapes of the measured and simulated magnetic field by calculating the correlation coefficient:

$$\rho = \frac{\sum_{i=1}^{n}(B_m^i - \overline{B}_m)\cdot(B_c^i - \overline{B}_c)}{\sqrt{Var(B_m)\cdot Var(B_c)}}$$

Here $Var(B)$ denotes the variance of a set of numbers B_i and $\overline{B}$ denotes their average. It should be pointed out that the correlation coefficient is insensitive to a multiplication factor scaling one set (of data points) relative to the other.

5. We determine the saturating field by minimizing the following expression with respect to the parameter ξ:

$$F(\xi) = \frac{1}{n}\sum_{i=1}^{n}(B_m(z_i) - \xi\cdot B_c(z_i))^2$$

6. The ξ that minimizes F is found and used to scale the saturating field used previously in the simulation to the new correct one.

This procedure proved very successful for determining the saturating field of the entrance magnets assuming that the 4 magnets (1st pair and 2nd pair) were identical. Therefore assuming that they all have the same saturating field we faced a one parameter problem. The quality of the fit is determined by two tests:

1. The correlation between B_m and B_c.
2. The minimum of the function $F(\xi)$.

Table 2 shows these results for the entrance and exit magnets and for the entire wiggler. It is clearly seen that the quality of the fit is not so good for the magnets at the exit since there we had a two parameter problem. At the exit there is an additional pair of magnets immediately after the wiggler periods, henceforth called

'symmetry magnets', which are identical in dimensions to the period magnets (full magnet) followed by two extra pairs of half size magnets (see Fig. 1). Thus at the exit there are two parameters (saturating fields) one for the first pair and another for the two successive pairs. In the first attempt we set the saturating field of the 'symmetry magnets' (the first pair out of the 3 exit magnet pairs) identical with that of the wiggler periods and the saturating field of the two successive pairs was set identical to that of the magnets at the entrance.

Table 2

	Correlation coefficient between B_m and B_c	square root of $F(\xi)$ at its minimum
Entrance	0.99968	5.55 Gauss
exit	0.99876	13.98 Gauss
entire wiggler	0.9874	192 Gauss
wiggler (periods only)	0.99	194 Gauss

The coincidence of the absolute magnitude of the sets is ensured by the requirement that $F(\xi)$ is minimized. Table 2 indicates that the shape of the measured magnetic field is close to that which was calculated by the El-Op simulation (good correlation coefficient). The last stage is to re-adjust the original saturation fields used in the simulation by multiplying them with the ξ that minimizes $F(\xi)$.

Determination of the saturation fields for the wiggler magnets

The saturating field of the wiggler magnets, for the El-Op simulations, was determined according to the requirement that the average of the absolute value of the field at the (local) maxima and minima will coincide with the average as obtained from the measurement with the Hall probe. The measurement of the field at the axis, using the Hall probe, is shown in figure 1. We calculated the average, $<B>$, of the field of the 26 largest negative peaks, B_n^i, and the absolute value of the 25 smallest positive peaks[1], B_p^i, which is given by:

$$< B >= \frac{1}{2}\left(\frac{1}{26}\sum_{i=1}^{26}\left|B_n^i\right| + \frac{1}{25}\sum_{i=1}^{25} B_p^i\right)$$

This calculation yields an average field amplitude on axis of *1936.64 Gauss*. We used in the El-Op simulation, a saturating field of *8094 Gauss* for the wiggler magnets and *8256 Gauss* for the additional magnets at the entrance and the exit. This gave an average field at the peaks of *1936.24 Gauss* which will be used henceforth. The reason we averaged the positive and absolute value of the negative peaks is that the measurement with the Hall probe might have been taken a little bit

[1] We skipped the maxima and minima near the edges so that the influence of the entrance and exit magnets is minimized.

off the wiggler's axis. This would have been the cause of an asymmetry between positive and negative fields and could lead to an error had we used only positive (or negative) peaks in the matching of the averages.

Determination of the saturating field for the longitudinal magnets:

The magnetic field of the longitudinal magnets is not supposed to vary along the z axis[2] therefore we had to use a different technique to evaluate their saturating fields. We measured the field of a pair of longitudinal magnets along the x axis, figure 6. The saturating field was determined by calculating the derivative of $B_y(x)$ with respect to x, as obtained from the measurement and equating it to the result obtained from the simulation. In this case also, the free parameter is the saturating field of the longitudinal magnet. We obtained a saturating field of *8840 Gauss* with this method. This saturating field produces a gradient of *-25 Gauss/mm* at the axis of the wiggler, taking into account the gaps between the longitudinal magnets.

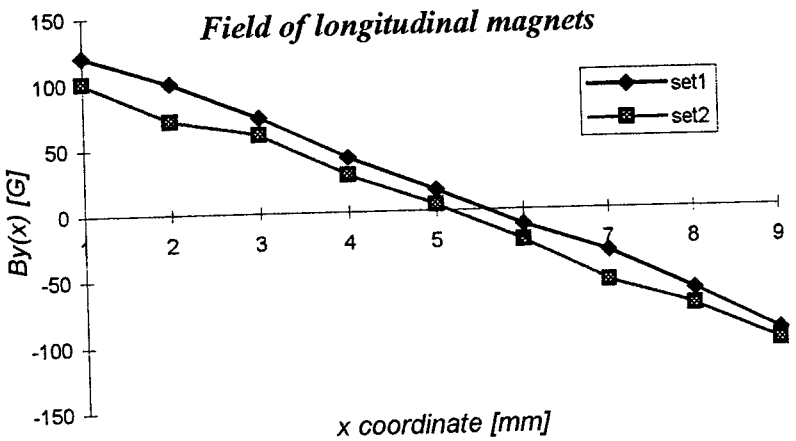

figure 6. Field of a pair of longitudinal magnets measured along the x axis.

Saturating field for the various magnets.

The saturating fields for the wiggler magnets that best coincide with the measurements are summarized in table 3. These values are recommended as reliable parameters for the simulations.

Table 3

	Saturating field (Gauss)
1st entrance magnets	9498.5
2nd entrance magnets	9498.5
Wiggler magnets	8094
Longitudinal magnets	8480
1st exit (symmetry) magnets	7655.4
2nd exit magnets	8983.8
3rd (last) exit magnets	8983.8

[2]In our wiggler we may witness a slight z dependence of the field since the long magnets do not cover the entire length of the wiggler and there is a small gap between the magnets along the wiggler's 114 cm.

A graph of the measurement vs. The simulation is shown in Fig. 6.1a for the entrance magnets and Fig. 6.1b for the exit magnets. The reader can see that for the vertical scale of the figure it is hardly possible to distinguish between the measurement and the calculation. Fig. 6.1c Shows the measurement and calculation of the field of the wiggler on the axis. The graphs do not coincide at the entrance and exit but we are not concerned about this since these sections were not used in the determination of the saturating fields for the wiggler magnets.

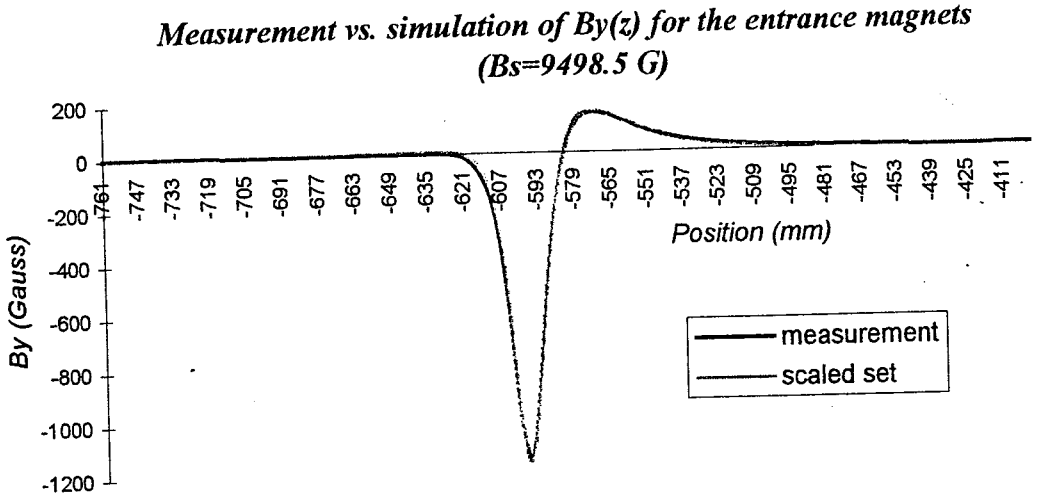

Figure 6.1a: Entrance magnets.

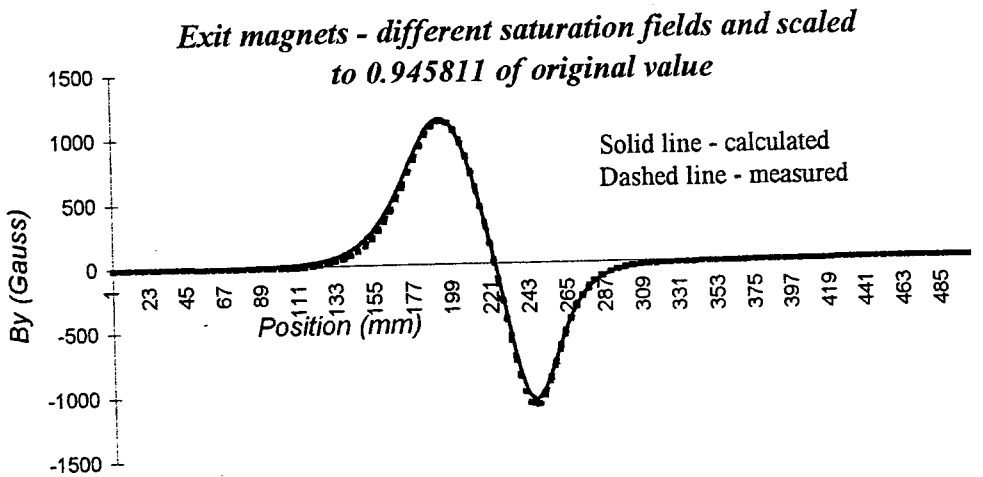

Figure 6.1b: Exit magnets.

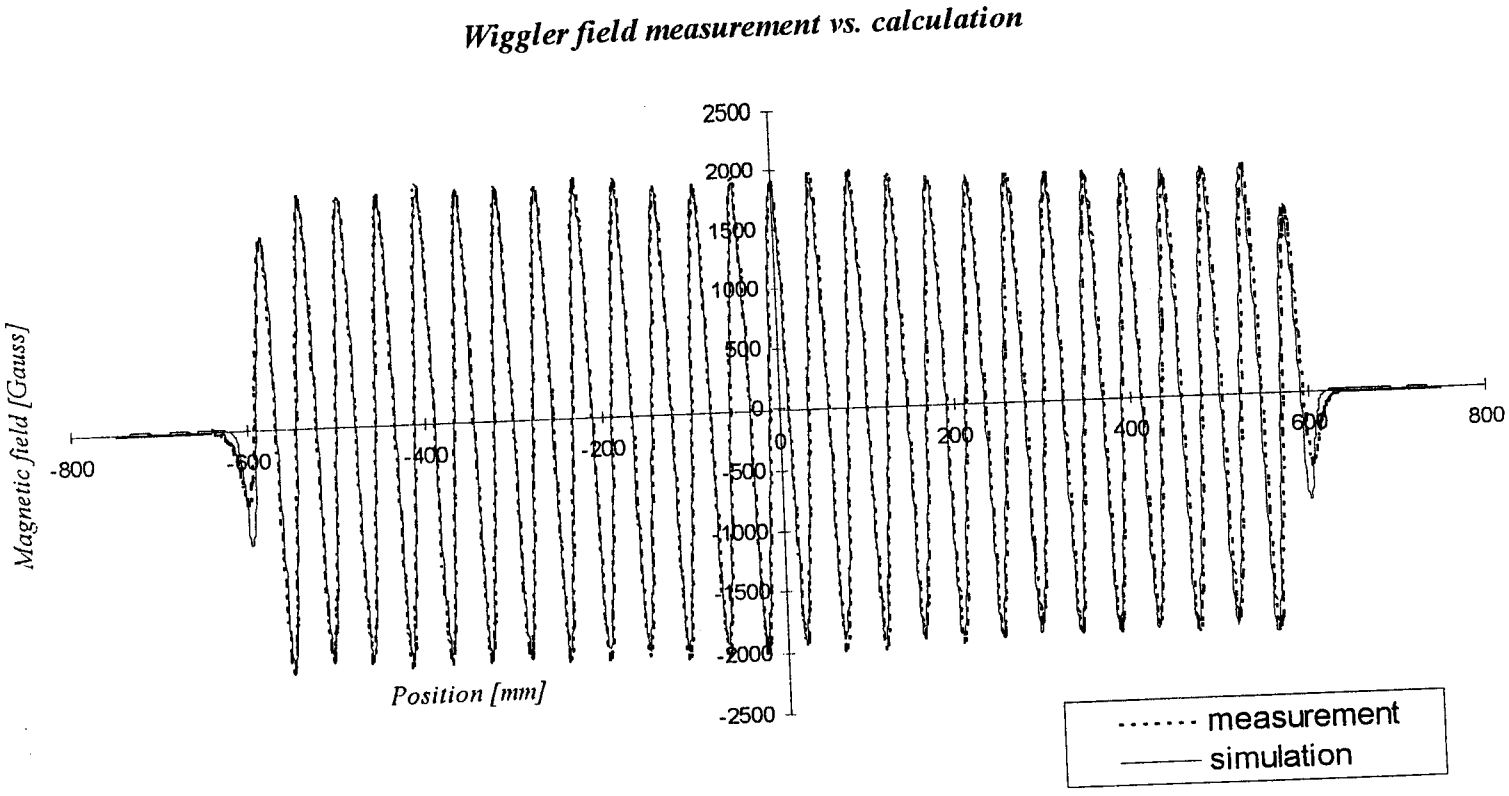

Figure 6.1c: Measurement vs. calculation of the field of the wiggler on the axis.

Optimization of the wiggler using the El-Op simulation

We decided to fix the distance of the correction magnets from the axis, at the entrance and exit of the wiggler according to the simulation results. Fig's 7-9 show the simulation results for optimal beam transport along the wiggler, also we include the parameters of the beam transport. Fig. 10 shows the double integral function of the magnetic field, $x(z)$, calculated on axis by El-Op for the suggested optimal transport conditions (Fig's. 7-9). This function is given in terms of the calculated field $B_c(z)$, the electron's mass m and charge e the entrance velocity V_0, and the relativistic constant γ by:

$$x(z) = +\frac{|e|}{m\gamma V_0}\int_{-\infty}^{z}\int_{-\infty}^{z'} B_c(z'')dz''dz'$$

Note that the double integral gives a result qualitatively different from the simulation. The later gives a straight electron path, parallel to the z axis (not accounting for the wiggling) whereas the double integral yields a path that diverges from the z axis at an angle of *20 mR* with exactly the same magnetic field. Outside the wiggler the divergence angle increases to almost *40 mR* due to the effect of the exit magnet. These results suggest that the pulse wire measurement does not give a reliable measurement of the electron path since the signal is proportional to the second integral of the field, which is different in our case (low energy, transverse field variation) from the real trajectories of the electron.

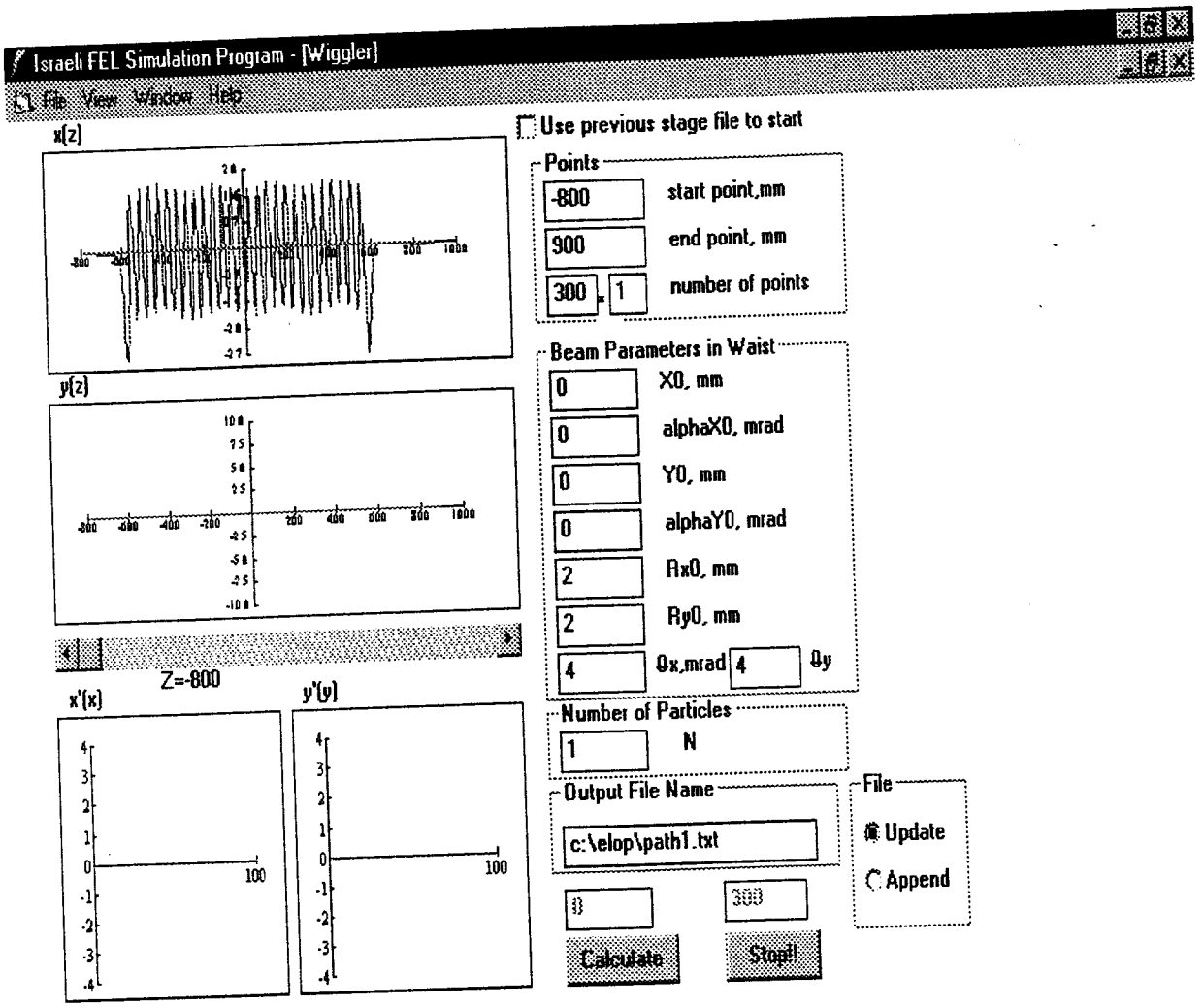

Figure 7: El-Op simulation of electron path for optimal transport.

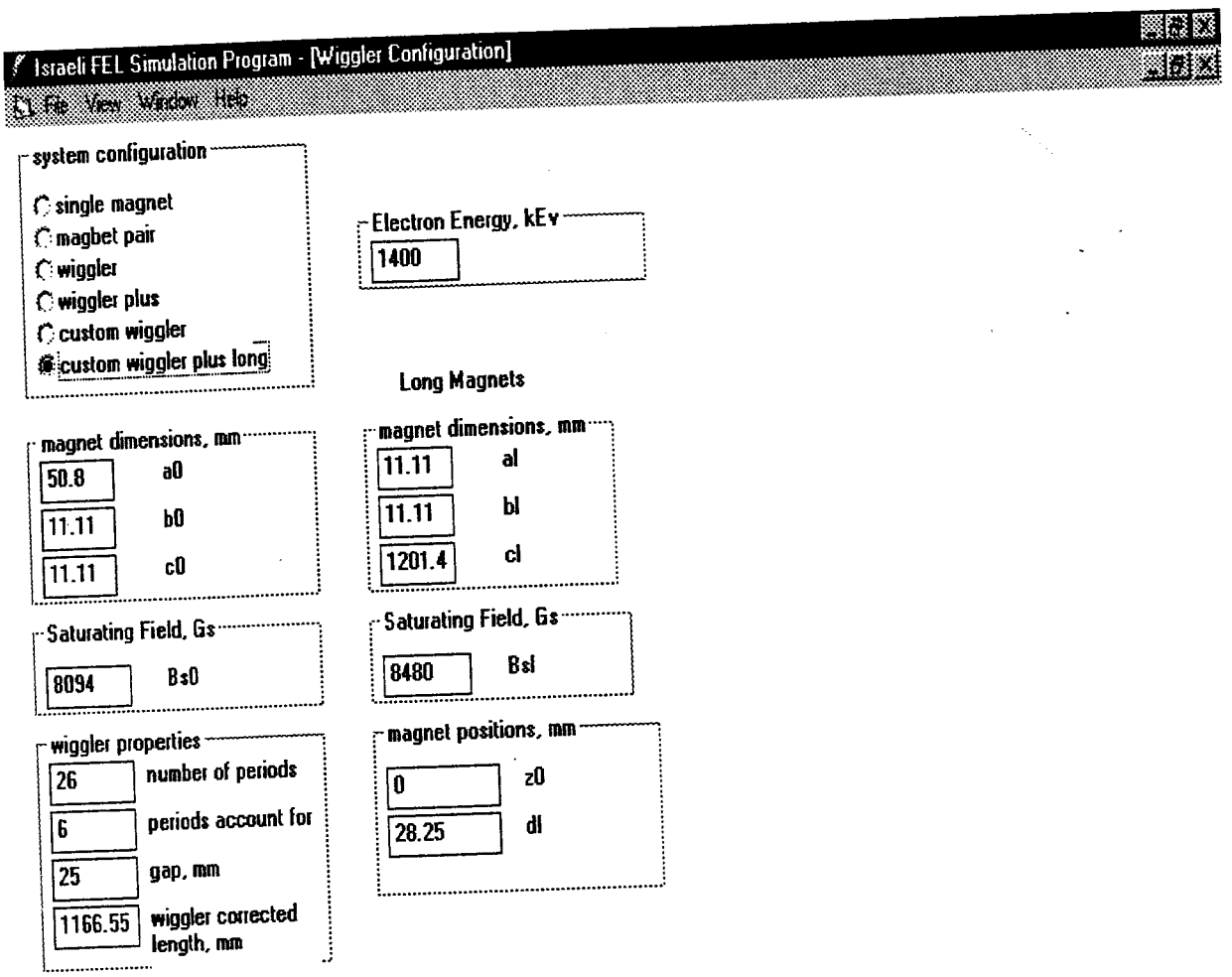

Figure 8: Wiggler configuration.

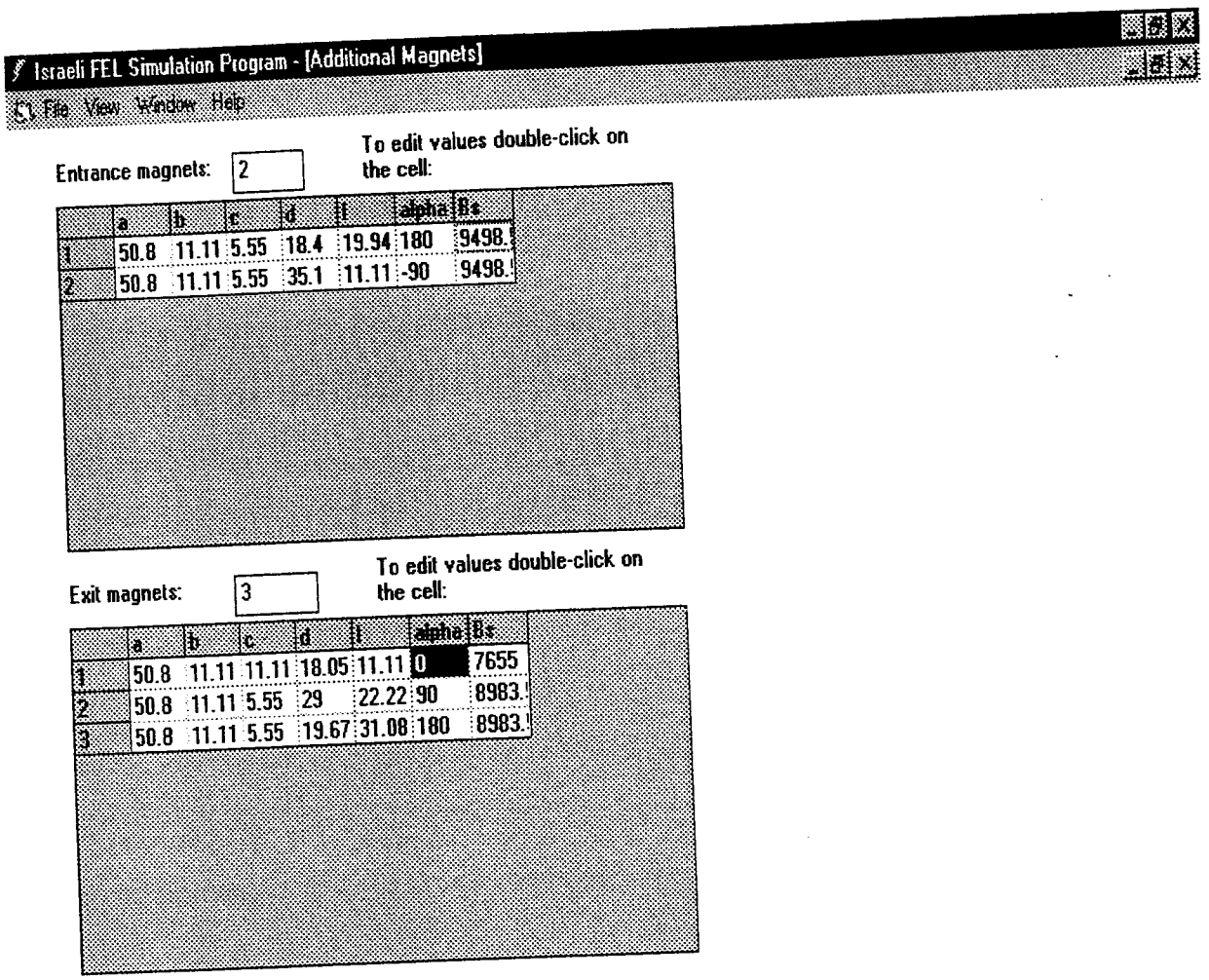

Figure 9: Arrangement of additional magnets at the entrance and exit for optimal transport (no betatron oscillation)

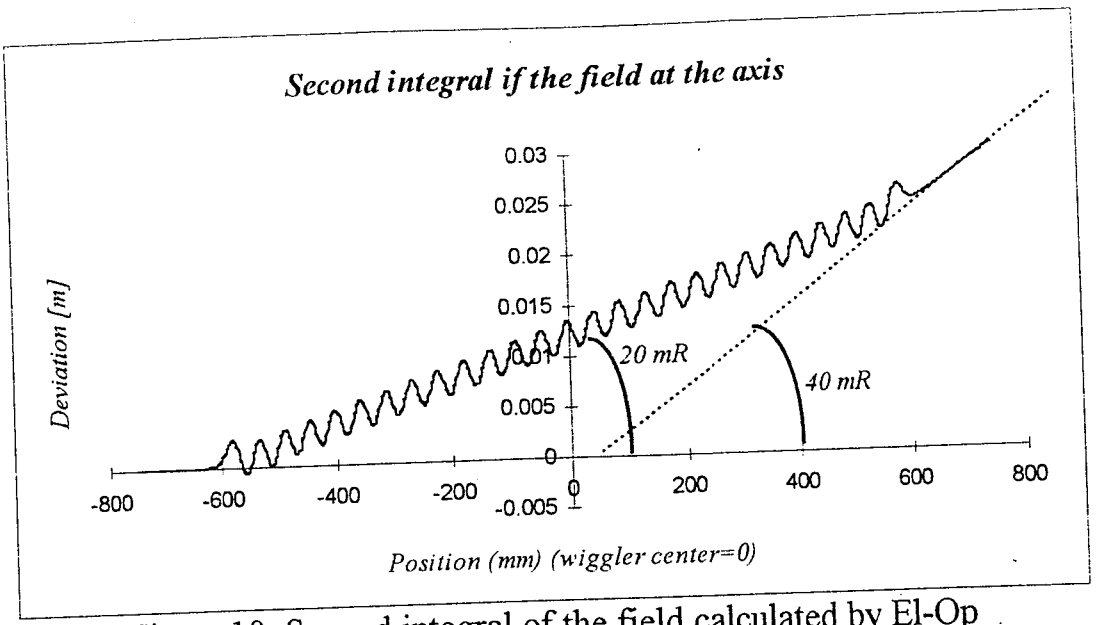

Figure 10: Second integral of the field calculated by El-Op

The wiggler arrangement

A practical problem that we face is that we can not adjust all the distances of the magnet pairs from the axis in accordance with the optimal values suggested by the simulation. In particular, the optimal distance between the second pair of entrance magnets and the axis, as dictated by the simulation is *d2=35.1 mm* (see fig. 9) but the aluminum support of the magnets does not permit a separation grater than 34.55 *mm*. This slight departure from the optimum position may be the cause of a small deviation angle and a parallel displacement of the beam. It is important to make sure that we can deal with this problem using the steering coils at the entrance to bring the beam back to the axis. The effect is evaluated as follows:
we choose an arbitrary point inside the wiggler (e.g. *z=0*) and calculate the coordinates and angles (of the electron) at that point, with El-Op, with the optimal parameters of Fig. 9 (including *d2=35.1 mm)*. These coordinates are then used as initial conditions when El-Op integrates the equations of motion from *z=0* backwards, but now with *d=34.55 mm* as in the real wiggler. The result of the integration gives a deviation angle of *0.407 mR* at the "exit" (which is actually the entrance) instead of the zero *mR* that were obtained had we left the distance between the second pair of magnets untouched. This result suggest that we may leave the distance as *34.55 mm* and correct the error with the help of the two steering coils that are planned to be placed at the entrance of the wiggler. The result of this simulation is shown in Fig. 11. The "exit" angle is too small to be resolved in the plot.

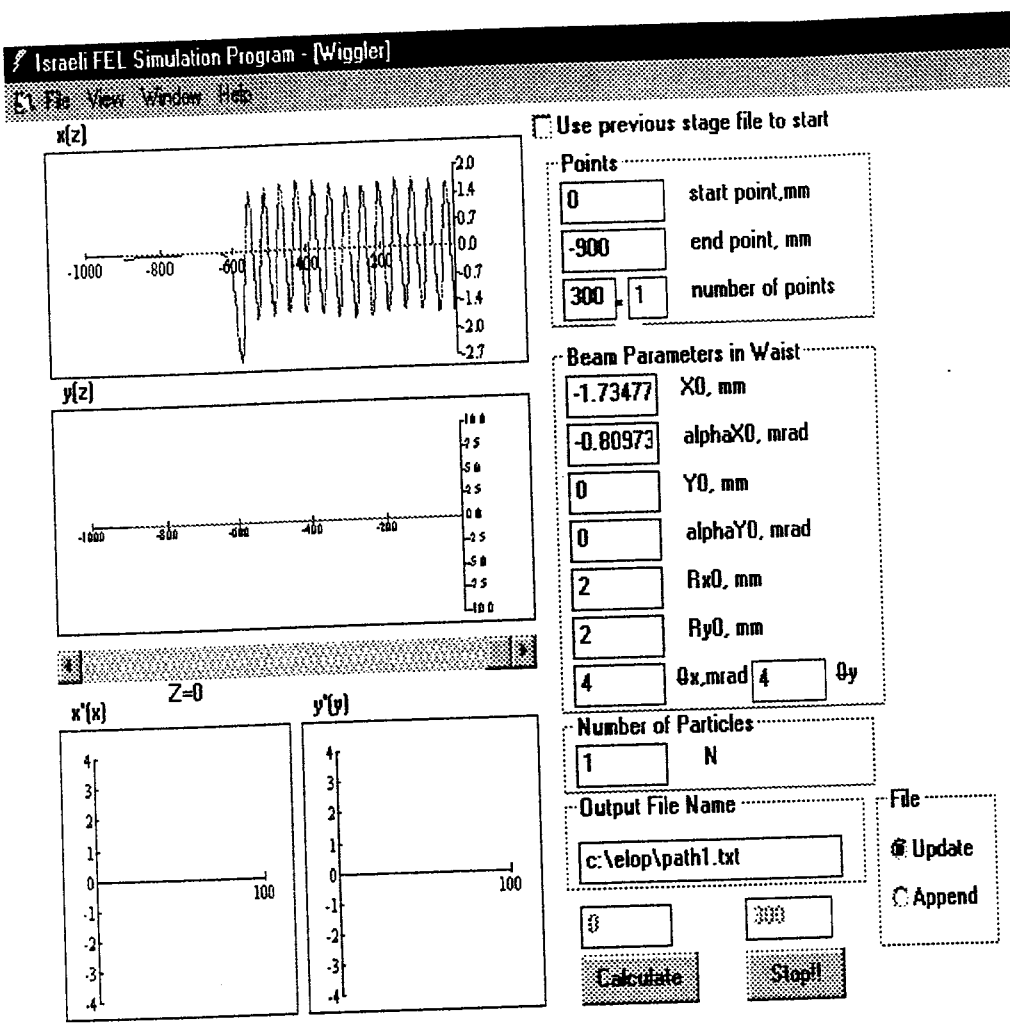

Figure 11: Simulation of the optimal electron trajectory, backwards for the real distance between the second pair of entrance magnets.

The final positions of the magnets are shown in Fig. 12 and the solution for these parameters is shown graphically in Fig. 13. Here again the it is difficult to observe the difference between this solution and the optimal solution in Fig. 7 since they are too close to each other. The second integral of the field for the feasible position of the entrance magnets arrangement is shown in Fig. 14. Note that there is no observable difference between Figs. 10 and 14.

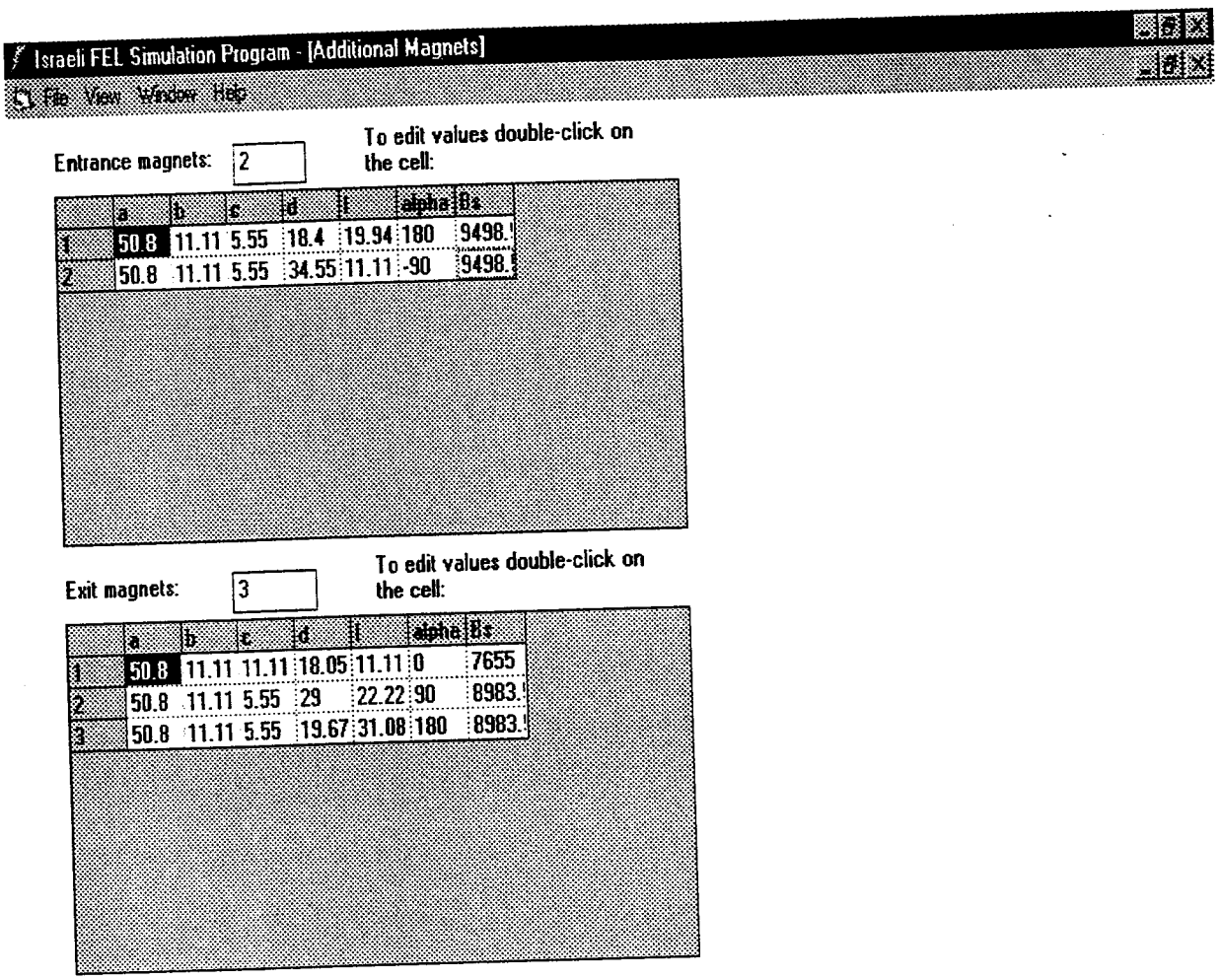

Figure 12: Final positions of entrance and exit magnets.

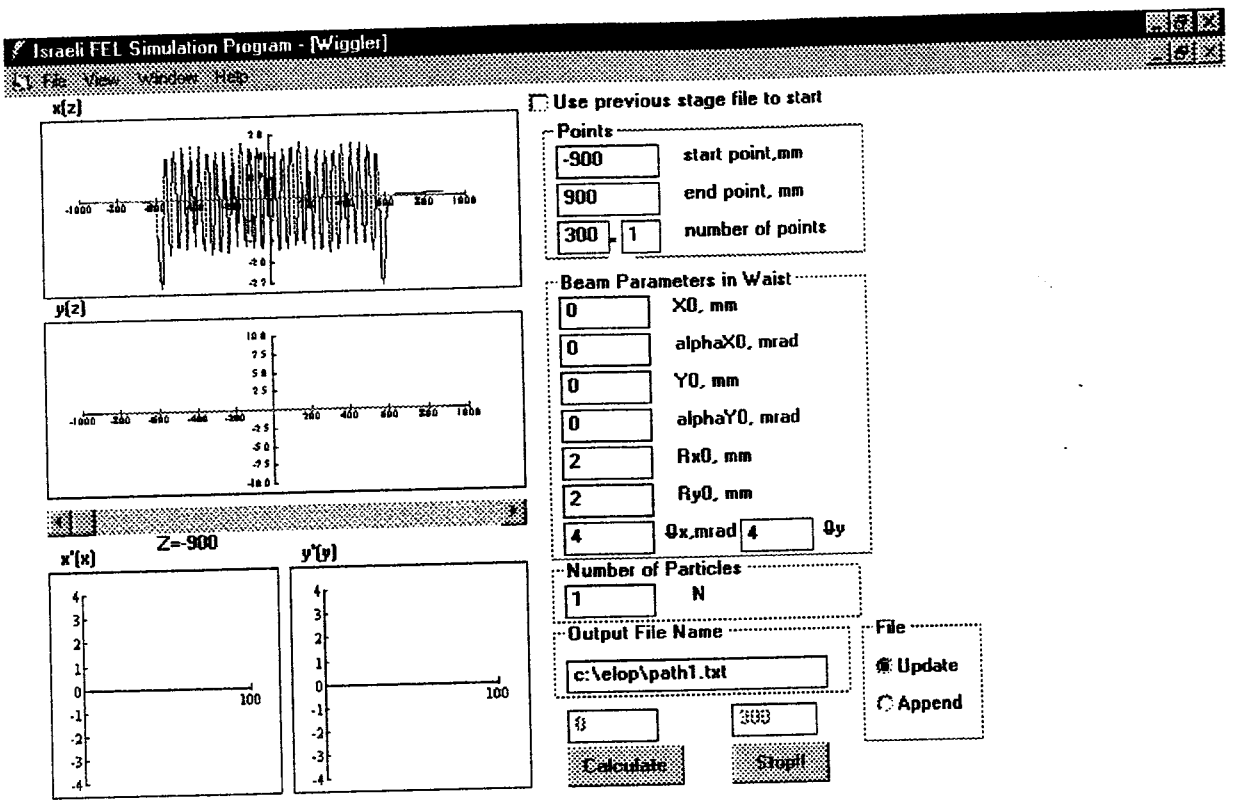

Figure 13: El-Op simulation of electron path for the final magnet arrangement.

Second integral if the field at the axis

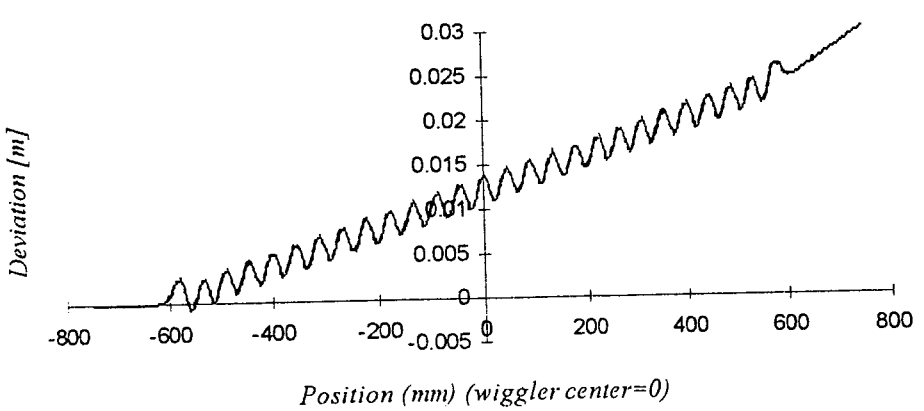

Figure 14: Second integral of the field for the feasible entrance magnet arrangement

Conclusions:

We can see by comparing figs. 7 and 10 that the precise solution to the electron path differs from the "simulation" of the path given by the pulsed wire technique. It follows that it would be wrong to arrange the correction magnets along the wiggler and the entrance and exit magnets in such manner that the pulsed wire setup gives a straight path using a long current pulse (path simulation). The correct procedure should be to determine the pulsed wire entrance and exit "angles" from the second integral of the field in the optimal transport configuration, and to make the corrections on the real wiggler so that the pulsed wire experiment gives us the same angles. This procedure may be difficult because of the sensitivity of the pulsed wire measurement to the exact wire position relative to the wiggler axis. Though it is not sensitive to misalignment in the y dimension, it is very sensitive to small misalignment (even 50 μm) in the x dimension where there is a strong gradient due to the longitudinal magnets.

Taking all this facts into account we deduce that the logical procedure would be to attain a straight second integral, with the pulsed wire setup, along the wiggler periods section by addition of small magnets. We will also try to adjust the wire position to the situation predicted theoretically: *20mR* angle at the entrance and *40mR* at the exit. If this will not be achieved, then corrections will be made in the real experiment with steering coils.